NeuroImage 109 (2015) 27–34

Contents lists available at ScienceDirect

NeuroImage

journal homepage: www.elsevier.com/locate/ynimg

Bilateral dorsal and ventral fiber pathways for the processing of affective prosody identified by probabilistic fiber tracking

Sascha Frühholz [a,b,*], Markus Gschwind [c,d], Didier Grandjean [a,b]

[a] Neuroscience of Emotion and Affective Dynamics Laboratory, Department of Psychology, University of Geneva, Geneva, Switzerland
[b] Swiss Center for Affective Sciences, University of Geneva, Geneva, Switzerland
[c] Laboratory of Neurology and Imaging of Cognition, Department of Neurosciences, University of Geneva, Geneva, Switzerland
[d] Neurology Service, Department of Clinical Neurosciences, Centre Hospitalier Universitaire Vaudois, Lausanne, Switzerland

ARTICLE INFO

Article history:
Accepted 2 January 2015
Available online 9 January 2015

Keywords:
Emotion
Prosody
Voice
DTI
Probabilistic fiber tracking
Auditory pathways

ABSTRACT

Dorsal and ventral pathways for syntacto-semantic speech processing in the left hemisphere are represented in the dual-stream model of auditory processing. Here we report new findings for the right dorsal and ventral temporo-frontal pathway during processing of affectively intonated speech (i.e. affective prosody) in humans, together with several left hemispheric structural connections, partly resembling those for syntacto-semantic speech processing. We investigated white matter fiber connectivity between regions responding to affective prosody in several subregions of the bilateral superior temporal cortex (secondary and higher-level auditory cortex) and of the inferior frontal cortex (anterior and posterior inferior frontal gyrus). The fiber connectivity was investigated by using probabilistic diffusion tensor based tractography. The results underscore several so far underestimated auditory pathway connections, especially for the processing of affective prosody, such as a right ventral auditory pathway. The results also suggest the existence of a dual-stream processing in the right hemisphere, and a general predominance of the dorsal pathways in both hemispheres underlying the neural processing of affective prosody in an extended temporo-frontal network.

Introduction

Cortical auditory processing involves several perisylvian regions, which are interconnected by different fiber pathways. Recent studies (Friederici et al., 2006; Rauschecker and Scott, 2009; Saur et al., 2008) have predominantly identified left hemispheric processing pathways within a dual-stream model of auditory processing (Hickok and Poeppel, 2007). They include ventral pathways from anterior superior temporal gyrus (STG) to the anterior inferior frontal gyrus (IFG) and dorsal pathways, which project to the posterior IFG via the posterior STG (Hickok and Poeppel, 2007; Rauschecker and Scott, 2009). Especially the dorsal pathway seems strongly left lateralized (Hickok and Poeppel, 2007). The ventral pathways convey sound-invariant meaning (Belin and Zatorre, 2000b; Rauschecker and Scott, 2009), such as speech semantics (Hagoort, 2005). The dorsal pathways serve sound-to-motor mapping (Saur et al., 2008) and the processing of temporal auditory sequences (Belin and Zatorre, 2000b; Rauschecker and Scott, 2009), which are also necessary for the understanding of speech syntax (Friederici et al., 2006). Compared to a predominant role of the left brain for syntacto-semantic processing (Specht, 2014), the emotional intonation in speech, that is the affective prosody, strongly, but not exclusively, activates regions in right STG and IFG (e.g. Alba-Ferrara et al., 2011; Beaucousin et al., 2007; Ethofer et al., 2006; Fruhholz et al., 2012). Thus, investigating the neural basis of affective prosody processing provides an ideal paradigm to investigate right hemispheric auditory pathways using diffusion-weighted imaging techniques together with functional magnetic resonance imaging.

These temporo-frontal pathways for affective prosody processing have been rarely studied (Ethofer et al., 2012; Glasser and Rilling, 2008), mainly pointing to a right dorsal pathway (Gharabaghi et al., 2009; Glasser and Rilling, 2008), but also providing evidence for the possibility of a right ventral pathway (Ethofer et al., 2012). However, these studies explored pathways, first, only for circumscribed temporal regions, second, without specifying frontal target regions, third, without quantifying the architecture of these pathways, and therefore without dissociating the different possible functional roles of these pathways (Ethofer et al., 2012; Glasser and Rilling, 2008). Taken together, these critical points might have led to a considerable underestimation of the importance and complexity of the temporo-frontal white matter pathway connectivity. Ventral and dorsal pathways, for example, are supposed to originate in multiple STG seed regions (Friederici, 2011; Fruhholz et al., 2012). Furthermore, these pathways probably terminate in the anterior as well as in the posterior IFG (Fruhholz and Grandjean, 2013b), serving to evaluate (Schirmer and Kotz, 2006) and to categorize

* Corresponding author at: Swiss Center for Affective Sciences University of Geneva, 9 Chemin des Mines, CH-1202 Geneva, Switzerland.
E-mail address: sascha.fruehholz@unige.ch (S. Frühholz).

http://dx.doi.org/10.1016/j.neuroimage.2015.01.016
1053-8119/

vocalizations (Romo et al., 2004), respectively. Thus, especially the use of multiple temporal and frontal seed and target regions might help to more comprehensively describe the extended structural temporo-frontal neural network underlying the processing of affective prosody.

Accordingly, using high-resolution fMRI we previously described several subregions in the bilateral IFG and in STG, which were differentially responsive to emotional compared to neutral prosody (Fruhholz et al., 2012). Especially, affective prosody elicits brain activity in several distributed subregions in right STG (Fruhholz and Grandjean, 2013a; Fruhholz et al., 2012) and right IFG (Fruhholz and Grandjean, 2013b), but these subregions have functional differences (Fig. 1). Especially, they show enhanced sensitivity to emotional compared to neutral prosody depending on the attentional focus *toward* (explicit attention) or *away from* (implicit attention) emotional cues in affective prosody. The right compared with left IFG showed a sensitivity to speech prosody during implicit attention, while left IFG subregions responded to affective prosody during both attentional conditions. All STG subregions showed a sensitivity to speech prosody both for the explicit and implicit attention condition, but right mid STG (mSTG) and left anterior STG (aSTG) showed stronger sensitivity during the explicit attention condition, whereby the latter regions showed a general main effect for the explicit compared with the implicit task, and thus might reflect a rather general evaluation of voices independent of the emotion. Furthermore, regions in the right posterior STG (fundus of the posterior superior temporal sulcus (fpSTS), posterior STG (pSTG)) and all left STG subregions were sensitive to the pitch and intensity variations in affective prosody, which are one of the main acoustic features of affective prosody (Banse and Scherer, 1996; Patel et al., 2011).

Based on these functional differences, we assumed different white matter fiber connections, which link different subregions in right STG and right IFG, probably similar to several STG–IFG fiber pathways described for the left hemisphere (Friederici, 2011). In the present study we therefore used diffusion-weighted imaging together with a probabilistic fiber tracking approach to investigate these temporo-frontal pathways, which might connect subregions in STG and IFG, which we observed previously (Fruhholz et al., 2012). Beside some left hemispheric pathways, we especially expected to find right dorsal and ventral pathways underlying the processing of affective prosody given the extended anterior to posterior distribution of right STG subregions.

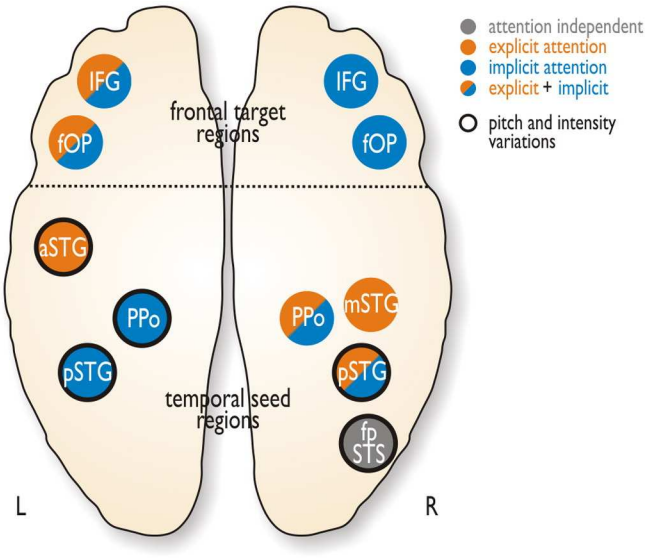

Fig. 1. Summary of the functional roles of the STG/STS and IFG subregions during the processing of affective prosody as found previously (Hickok and Poeppel, 2007). Some of these activations were found independent of the attentional focus, during both the explicit and the implicit attention condition, or were especially enhanced during the explicit or implicit attention task. Additionally, some of these regions were sensitive to pitch and intensity variations of affective prosody (encircled in black).

Materials and methods

Participants

To investigate bilateral temporo-frontal pathways for the processing of affective prosody, we recorded diffusion-weighted imaging data in participants, who listened to affective prosody in a previously described experiment (Fruhholz et al., 2012). Seventeen healthy participants took part in the experiment. Data from two participants had to be excluded from the analysis because of signal artifacts in the diffusion-weighted data. The remaining sample consisted of three males and twelve females, with a mean age of 25.12 years ($SD = 4.95$, age range 20–38 years). All participants were native French speakers, were right-handed, and reported to have normal or corrected-to-normal vision, and to have no hearing disabilities. No subject presented a psychiatric or neurological medical history. Subjects gave informed and written consent for their participation in accordance with the ethical and data security guidelines of the University of Geneva. The experiment was approved by the local ethics committee of the University of Geneva.

MRI scanning

Images were recorded on a 3T Siemens Trim Trio System (Siemens, Erlangen, Germany) equipped with a 32-channel head coil using parallel imaging (GRAPPA factor 2). First, two repetitions of monopolar diffusion-weighted images (Stejskal-Tanner; TR/TE = 8200/82 ms, vocal size 2 mm^3, 65 slices) were performed along 30 independent directions, including a *b*-value of 1000 s/mm^2. A reference image with no diffusion weighting ($b = 0$ s/mm^2) was also obtained during each diffusion-weighted acquisition. Second, a high-resolution, magnetization-prepared rapid acquisition gradient echo (MPRAGE) T1-weighted sequence (TR/TE/TI = 1900/2.27/900 ms, FoV 296 mm, voxel size 1 mm^3, 192 slices) was obtained in sagittal orientation to obtain structural brain images. Finally, functional images were recorded using high-resolution T2*-weighted EPI images (TR/TE/TA = 10,000/30/8250 ms, voxel size 1.5 × 1.5x2 mm, 25 slices).

Stimuli and procedure

A full description of the stimuli and the experimental setup can be found here (Fruhholz et al., 2012). In short, we presented four speech-like but meaningless words ("*molen*", "*belam*", "*nikalibam*", "*kudsemina*"), which were spoken in either a neutral or an angry tone by two male and two female actors. The same stimuli were presented during blocks, which varied according to the focus of attention. In two blocks participants were asked to make explicit prosody discriminations (*neutral* or *angry*; referred to as "explicit attention"). In another two blocks participants were asked to discriminate the gender of the voices (*male* or *female*; referred to as "implicit attention"), where the emotional intonation of words was assumed to be processed on an implicit level.

Region of interest (ROI) selection for seed regions

With the above described experimental procedure, we previously identified several subregions in the left and right superior temporal cortex (STC, consisting of STG and STS) and two subregions in the bilateral IFG resulting from the comparison of angry and neutral voices across both attention levels, but also for this comparison within each of the explicit and the implicit attention condition (Fig. 1) (Fruhholz et al., 2012). Here we used these regions as seed and target regions for probabilistic fiber tracking in order to establish the white matter connectivity between these regions. We took three subregions in the voice-sensitive cortex of the left hemisphere (pSTG [MNI *xyz* −68 −27 6], planum polare (PPo) [−50 −10 4], aSTG [−56 11 −10]), and two IFG subregions, one located more posterior in the frontal operculum (fOP; BA 44; [−51 13 14]), and one more anterior in the IFG (BA 47; [−44 29

0]) (Fig. 2B). In the right hemisphere we used the previously found four STG subregions (fpSTS [45 −34 4], pSTG [69 −22 4], mSTG [66 −3 2], PPo [53 −4 −4]), and two IFC subregions, one located more posteriorly in the fOP (BA 44; [48 13 −2], and one more anteriorly in the IFG (BA 47, [51 32 −2]) (Fig. 3B). Note that all four right STG subregions except PPo, were located in the voice-sensitive cortex, as defined by a standard voice localizer scan (see Belin and Zatorre, 2000a).

Image processing and data analysis

Diffusion-weighted data were preprocessed and analyzed using the FSL software package (version 4.1.6; www.fmrib.ox.ac.uk/fsl). The data were corrected for eddy currents and motion, and subsequently averaged across the two acquisitions. At each voxel, we estimated the two most likely diffusion directions by using Bayesian estimation as implemented in the FDT toolbox, including a model that accounts for the possibility of crossing fibers within each voxel (Behrens et al., 2007). The estimation was performed in native diffusion space. An exclusion mask was applied covering the whole non-brain space, especially taking into account the lateral sulcus to avoid spurious temporo-frontal shortcuts.

In order to initiate fiber tracking from the fMRI derived activation peaks, MNI locations of group activations were transformed in two steps. First, peak activations were first slightly moved to the nearest

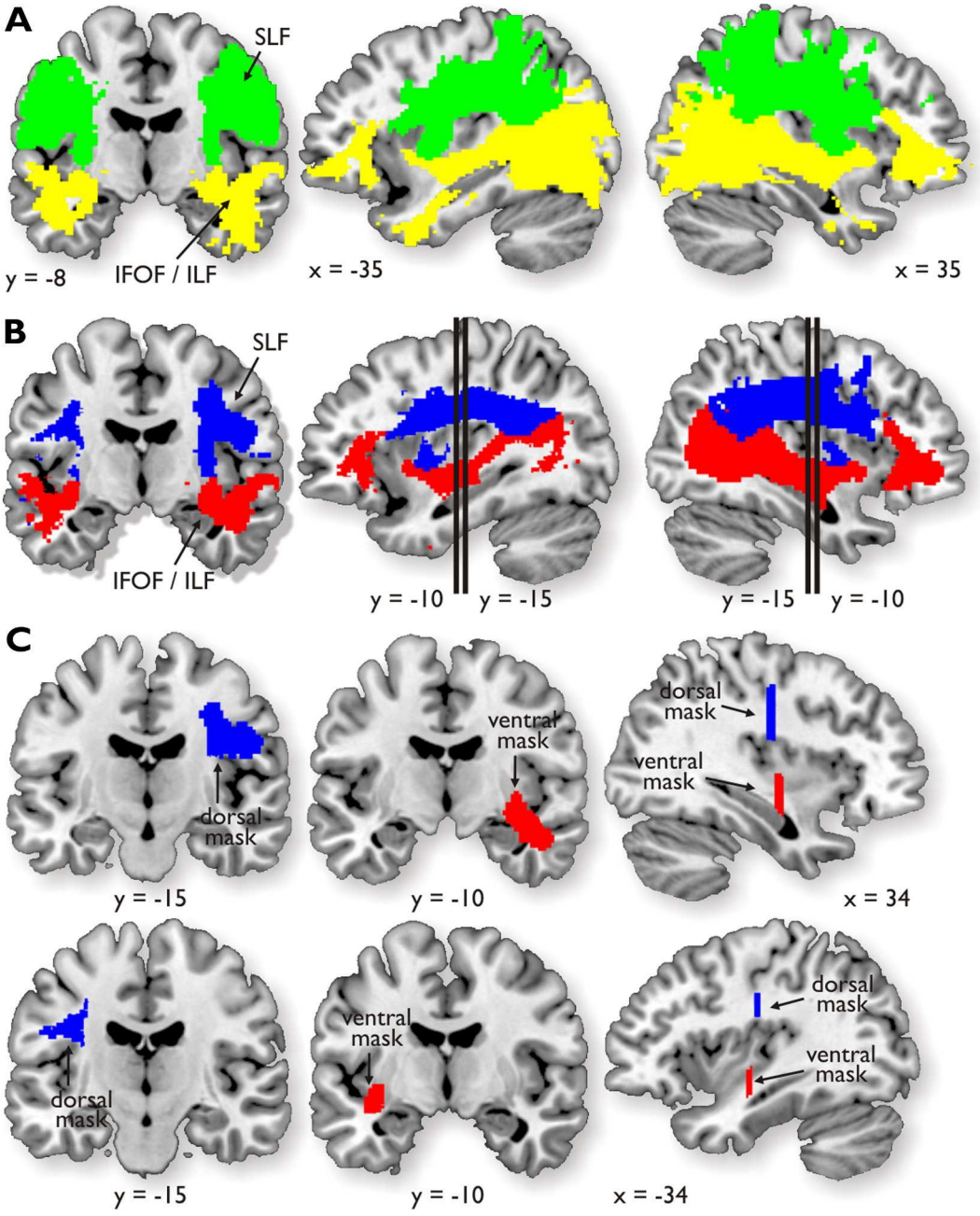

Fig. 2. Dorsal and ventral pathway waypoint mask. (A) In a first step, we defined one mask consisting of the superior longitudinal fasciculus (SLF) mask (green), and another mask white-matter mask (yellow) consisting of the inferior longitudinal fasciculus (ILF) and the inferior-occipito-frontal fasciculus (IFOF). All masks were taken from the JHU white-matter tractography atlas. (B) The spatial overlap between the general fiber pathway mask (i.e. containing all fiber pathways identified here) and the SLF mask resulting from the procedure in A served the definition of the dorsal pathway (blue), while the overlap between the general fiber pathway mask and the combined ILF/IFOF mask served the definition of the ventral pathways (red). (C) Finally, from the ventral and the dorsal pathway masks resulting from B, we took single slices at the coronal level of $y = -15$ and $y = -10$ to define waypoint masks for quantitative fiber tracking of the dorsal (blue) and the ventral pathway connections (red), respectively, in order to calculate the pathway probability (PP).

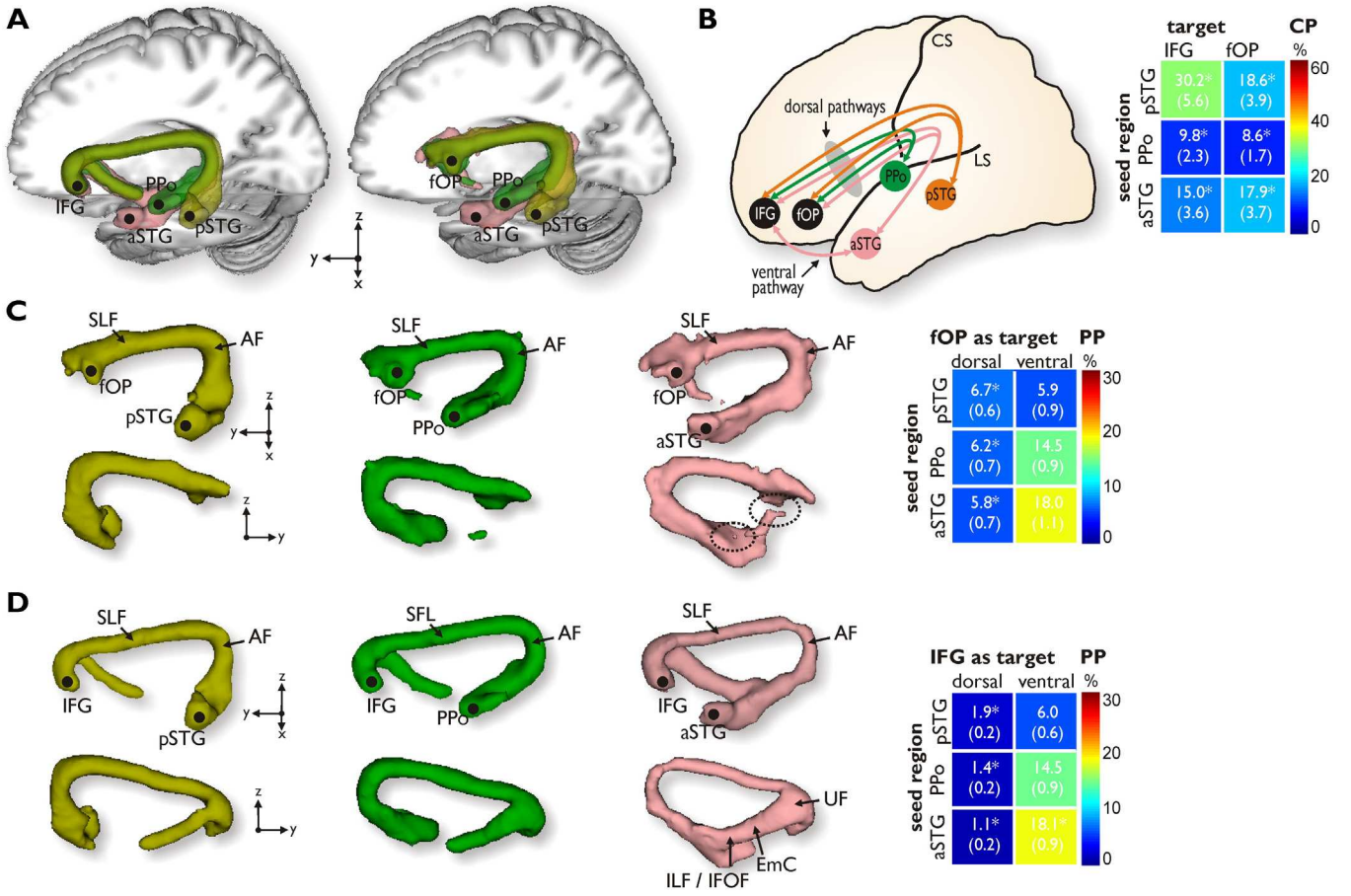

Fig. 3. Probabilistic fiber pathways for the left hemisphere. (A) Probabilistic fiber pathways between the three left STG areas (pSTG, PPo, aSTG) as seed regions and the IFG (left panel) and the fOP (right panel) as target regions. (B) Schematic image of the left dorsal and ventral fiber pathways originating from the three STG subregions and the two IFG subregions. The right panel shows connection probabilities (CP) between each temporal seed region and the frontal target regions (*asterisks indicate PPs for existing pathways as shown in C and D). (C) Temporo-frontal pathways separately for all three temporal seed regions and the fOP as the frontal target region. The encircled region (dotted line) shows an area of missing continuation of fiber pathways due to inconsistent pathway probabilities across participants. The right panel shows the pathway probabilities (PP) for each temporal seed region, indicating the probability of the connection to the frontal target regions taking the dorsal or the ventral pathway (see Fig. 1). (D) Temporo-frontal pathways for all three temporal seed regions and the IFG as the frontal target region. Abbreviations: *AF* arcuate fasciculus; *aSTG* anterior superior temporal gyrus; *CP* connection probability; *CS* central sulcus; *EmC* extreme capsule; *fOP* frontal operculum; *IFG* inferior frontal gyrus; *ILF* inferior longitudinal fasciculus; *IFOF* inferior fronto-occipital fasciculus; *LS* lateral sulcus; *PP* pathway probability; *PPo* planum polare; *pSTG* posterior superior temporal gyrus; *SLF* superior longitudinal fasciculus.

gray–white matter boundary in MNI space. Second, these peak locations were then back-transformed to the native diffusion space of each individual by using the inverse normalization parameters, obtained by the segmentation of the anatomical images using SPM8 (www.fil.ion.ucl.ac.uk/spm). Prior to this segmentation and inverse warping, the anatomical image was coregistered to the fractional anisotropy image that resulted from the estimation of the diffusion directions (see above). This coregistration was done using FLIRT in FSL. After back-transforming the peak locations from MNI to native space. A 4 mm radius sphere was then placed around each peak coordinate and the volume of voxels that individually overlapped with the white matter in each participant served as seed and target regions for the probabilistic fiber tracking (see Gschwind et al., 2012). The resulting volume of voxels did not include voxels that overlapped with the exclusion mask of nonbrain volume (see above), and were as follows for left regions in fOP (M_{vol} = 124 mm^3, SEM 11), IFG (M_{vol} = 111 mm^3, SEM 10), pSTG (M_{vol} = 38 mm^3, SEM 5), and aSTG (M_{vol} = 86 mm^3, SEM 5), PPo (M_{vol} = 68 mm^3, SEM 10), as well as for right regions in fOP (M_{vol} = 81 mm^3, SEM 6), IFG (M_{vol} = 77 mm^3, SEM 12), fpSTS (M_{vol} = 126 mm^3, SEM 3), pSTG (M_{vol} = 53 mm^3, SEM 5), mSTG (M_{vol} = 40 mm^3, SEM 5), and PPo (M_{vol} = 63 mm^3, SEM 5).

We choose to define seeds on group-based peak activations back-transformed to the individual space of each participant. The fundamental dependency of the activation cluster size on the chosen statistical threshold, and thus a principal impossibility to determine the exact extent of a functional region, motivated our approach to define seed ROIs with spheres of the same size, centered on the peak of the group cluster activations. Although relying on group-level analysis using normalized brain anatomy can sometimes lead to activations that are not consistently found in each and every subject of the group, and because the peak represents an average result, it may not provide the exact localization of maximal responses in each individual brain. However, this approach is consistent with a large body of neuroimaging research (Saur et al., 2008), and seems unlikely to introduce biases in our results.

From each seed voxel, we sent out 25,000 samples (step length 0.5 mm, curvature threshold 0.2) mapping the probabilistic connectivity pattern. The resulting maps were thresholded at 5% and normalized to MNI standard space using nonlinear transformation warp fields (provided by the TBSS pipeline; Smith et al., 2006). Group analysis was performed on group connectivity probability maps (binarized and summed) across participants. The resulting group maps were thresholded at a level of >7 (=53.3%), indicating that at least eight of the 15 subjects consistently showed the respective connecting fiber tracks (Gschwind et al., 2012).

The connectivity analyses were performed in two stages. The first analysis stage included probabilistic fiber tracking in the left hemisphere between each of the three regions in the STG as seeds and each of the two regions in the IFC as targets, thus resulting in six different

connectivity pairs (3 seed regions × 2 target regions) (Gschwind et al., 2012). Fiber tracking was performed in both directions, from seed to target and backwards, and the resulting connectivity maps were averaged such that only fiber connections were kept that were present both in the forward and in the backward probability map (i.e. which were nonzero in both maps). Group connectivity maps were then generated as described above. The same steps were performed on the four STC and the two IFC subregions in the right hemisphere. The first analysis stage revealed dorsal and ventral pathways between the different subregions in the STC and the IFC in both hemispheres.

In order to estimate the relative connectivity of the dorsal and the ventral pathways, we then conducted two additional analyses on the second stage. We included waypoint masks for the dorsal and the ventral pathway, which constrained the tracking algorithm to fibers that only passed through the respective masks (Fig. 2). These dorsal and ventral waypoint masks were generated as follows. First, we defined superior longitudinal fasciculus (SLF) masks taken from the JHU white-matter tractography atlas at a probability threshold of 100% (Hua et al., 2008). The SLF is the main dorsal longitudinal fiber bundle connecting posterior and anterior brain regions, as has been frequently reported to contain fiber connections between regions involved in auditory communication (Hua et al., 2008) (Fig. 2A). Furthermore, we defined a white-matter mask by combining the inferior longitudinal fasciculus (ILF) and the inferior fronto-occipital fasciculus (IFOF) taken from the JHU atlas, as the main ventral longitudinal fiber bundles (Friederici, 2011; Saur et al., 2008). Subsequently, we created a general white-matter pathway mask by summing up all fiber pathways from all seed and target regions across all participants. The spatial overlap between this general fiber pathway mask and the SLF mask resulting from the procedure in the first step served the definition of the dorsal pathway (Fig. 2B). The overlap between the general fiber pathway mask and the combined ILF/IFOF mask served the definition of the ventral fiber pathways. Finally, from the dorsal and ventral fiber pathway masks we took single slices at the coronal levels of $y = -15$ and $y = -10$ to define waypoint masks for the dorsal and the ventral pathways, respectively (Fig. 2C). These slices were taken at a coronal position where the dorsal and ventral pathway masks showed highest consistency in terms of a posterior-to-anterior directionality (Friederici, 2011; Saur et al., 2008). All three steps were performed for each hemisphere separately. The resulting waypoint masks were transformed to each participant's native space for probabilistic fiber tracking in native space.

The connectivity probability (CP) between a given pair of ROIs was calculated as the average number of successful samples (i.e. reaching the target regions) of the 25,000 samples sent out per each effective voxels (i.e. those voxels that were located in the white matter) in the seed and a target ROI (Croxson et al., 2005; de Wit et al., 2012; Gschwind et al., 2012). The number of successful samples was then normalized by the total number of all successful samples across all investigated seed and target regions for each subject in each hemisphere. The pathway probability (PP) between two ROIs was calculated as the number of successful samples between seed and target ROI specifically for the dorsal or the ventral pathway (Fig. 2), again normalized across the sum of all pathways in each hemisphere. All CP and PP data were normally distributed as indicated by nonsignificant Kolmogorov–Smirnov tests on all one-to-one temporo-frontal connections in each hemisphere (all Ps > 0.174). The CP values were subjected to a random-effects repeated-measures analysis of variance (ANOVA) with the within-subject factors *temporal seed* (3 ROIs) and *frontal target* (2 ROIs) for the left hemisphere, and to a 4 × 2 ANOVA for the right hemisphere, respectively. Significant main effects were followed by Bonferroni-corrected planned comparisons between the factor levels, and significant interactions were followed by a post hoc Student *t*-test between the factor combinations of interest. Each ANOVA was accompanied by a Mauchly test of sphericity. In the case of a significant Mauchly test, we applied Greenhouse–Geisser correction to the degrees of freedom and the *P*-values of the comparison of interest. *T*-tests were computed for those pathway probabilities of connections (right fpSTS-IFG, left aSTG–IFG) that showed both a dorsal and a ventral pathway.

Results

Using high resolution fMRI and minimal smoothing, we have recently provided a detailed mapping of the regions, which were sensitive to speech prosody conveyed by emotional vocalizations, including several subregions in the bilateral STG and the IFG (Fig. 1). Here, we tested for white matter connectivity between these regions and therefore performed probabilistic fiber tracking separately for the left and the right hemisphere pairwise between all ipsilateral STG and IFG subregions.

Concerning the left hemispheric pathways (Fig. 3), we found that all frontal target regions were targeted with equal strength in terms of connection probability (CP) by the STG seed regions indicated by a nonsignificant effect for the factor *frontal target* ($F_{1,14} = 0.592$, $P = 0.455$). The anterior STG (aSTG) was connected to the IFG via a strong ventral pathway consisting of the inferior longitudinal fasciculus (ILF) and the inferior fronto-occipital fasciculus (IFOF) in its posterior portion, and the extreme capsule (EmC) in the anterior portion (Fig. 5A), as confirmed with a standard white matter atlas (Catani and Thiebaut de Schotten, 2008). The identification of the EmC was also based on the anatomical knowledge especially regarding its topographic distinction from the close external capsule (EC). The EmC is a cortico-cortical association pathway, while the EC belongs to the cortico-striatal fiber system (Makris and Pandya, 2009). The aSTG was also connected to the IFG via a dorsal pathway, but the aSTG–IFG connectivity displayed a higher pathway probability (PP) via the ventral compared with the dorsal pathway ($t_{14} = 18.874$, $P = 2.35 \times 10^{-11}$) (Fig. 3D). The aSTG finally showed a connection to the left frontal operculum (fOP) by dorsal pathways. Unlike the aSTG, the left polare plane (PPo) and the posterior STG (pSTG) were connected to both the IFG and the fOP only via dorsal pathways. The strongest CP originating from the STG seed regions was actually found for the pSTG and targeting all frontal regions (main effect for the factor *temporal seed*: $F_{1.44,20.16} = 7.469$, $P = 0.007$, Greenhouse–Geisser (GG) corrected), especially for the comparison of the pSTG compared with the PPo (planned posthoc comparison: $P = 7.74 \times 10^{-4}$).

We also observed several fiber pathways in the right hemisphere (Fig. 4). All frontal regions were targeted with equal CP indicated by a nonsignificant main effect for the factor *frontal target* ($F_{1,14} = 2.979$, $P = 0.106$), but different seed regions had differential CP to these frontal target regions indicated by a significant effect for the factor *temporal seed* ($F_{1.11,15.47} = 415.785$, $P = 3.05 \times 10^{-31}$, GG corrected). Specifically, we found that while all subregions in the STG were connected to the right fOP via dorsal pathways, only the most posterior region in the right fundus of the posterior superior temporal sulcus (fpSTS) was connected to the right IFG via equally strong dorsal and ventral pathways (i.e. indicated by a nonsignificant effect of for the comparison of the dorsal and ventral PP; $t_{14} = 0.023$, $P = 0.982$) as well as to the fOP via a dorsal pathway. The ventral pathway consisted of the ILF/IFOF in the posterior part and the EmC in the anterior part (Fig. 5B). The fpSTS revealed the strongest CP to frontal target regions compared with all other STC seed regions (planned post-hoc comparisons for the main effect of the factor *temporal seed*: all Ps < 1.85×10^{-10}), and showed a nonsignificant trend toward a higher CP to fOP than to IFG indicated by a *temporal seed* × *frontal target* interaction ($F_{1.01,14.19} = 4.694$, $P = 0.047$, GG corrected; post hoc: $t_{14} = 2.054$, $P = 0.059$). The right PPo, mid STG (mSTG), and pSTG were connected only to the fOP via dorsal pathways. The least CP was found for the mSTG, especially as compared with the pSTG and the PPo (planned post-hoc comparisons for the main effect of the factor *temporal seed*: all Ps < 0.041).

Finally, we extracted microstructural properties of the white matter (Pierpaoli et al. 1996), including the mean FA and mean diffusivity (MD) for all reported pathways. Table 1 shows the mean values for these connections, averaged for both fiber-tracking directions. All these values

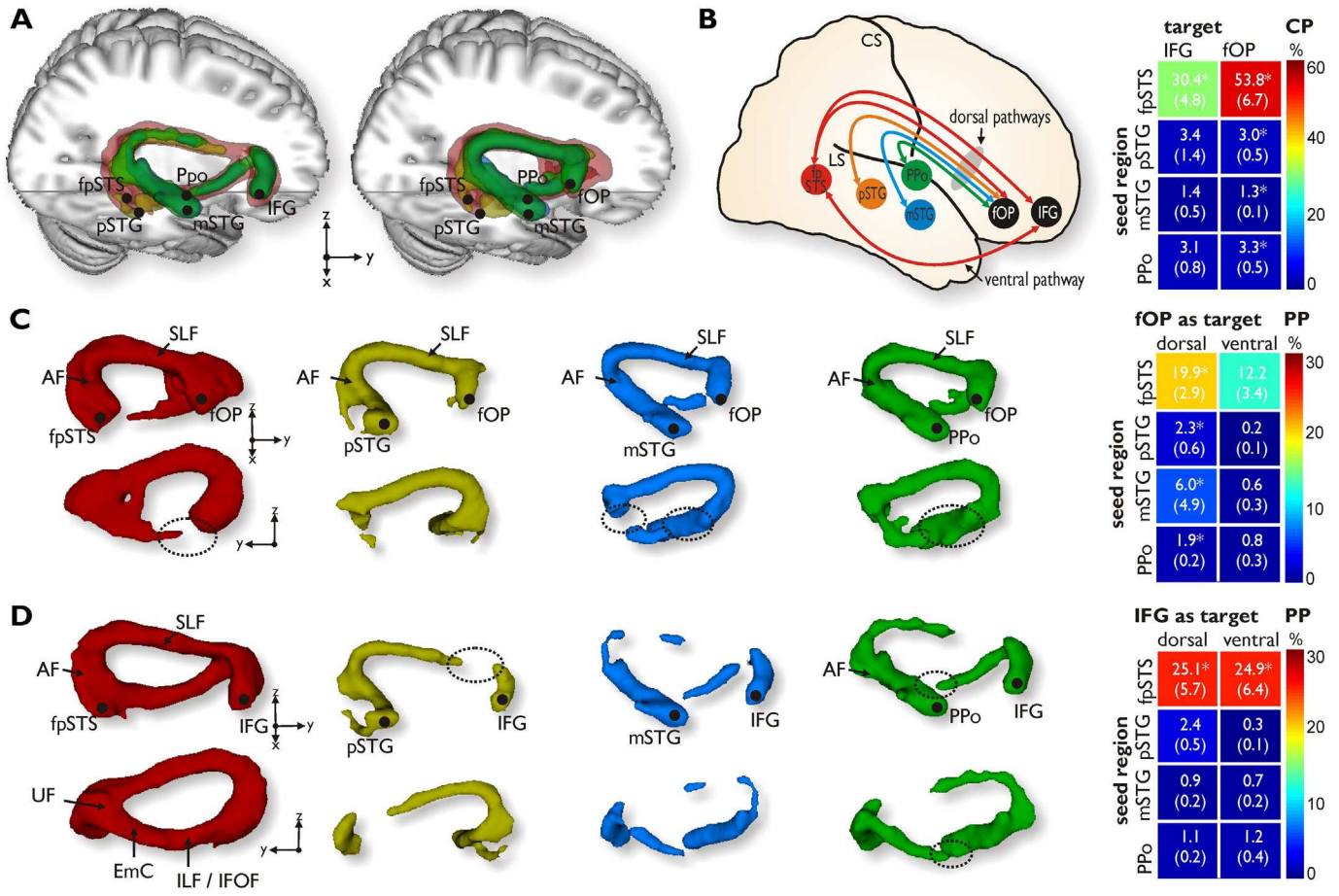

Fig. 4. Probabilistic fiber pathways in the right hemisphere. (A) Probabilistic fiber pathways between the four right STG seed regions (fpSTS, mSTG, PPo) and the IFG (left panel) and the fOP (right panel) as target regions. (B) Schematic image of the right dorsal and ventral fiber pathways from the four STG subregions and the two IFC subregions. (C) Temporo-frontal pathways separately for all four STG seed regions and the fOP as the frontal target region. (D) Temporo-frontal pathways for all four STG seed regions and the IFG as the frontal target region. For general abbreviations, see Fig. 1; *fpSTS* fundus of posterior superior temporal sulcus; *mSTG* mid superior temporal gyrus.

were in the range typically reported for small white-matter tracts in cortical proximity (Wahl et al. 2010), thus supporting the quality and reliability of our data.

Discussion

The present results revealed several new findings, mainly pointing to bilateral dorsal and ventral temporo-fronto pathway connections of regions involved in processing affective prosody. The dorsal pathway mainly consisted of fiber bundles belonging to the AF and the SLF, whereas the ventral pathway was composed of parts of the ILF, IFOF, and the EmC. First, we revealed some left-hemispheric temporo-frontal connections for affective prosody processing, especially dorsal connection between the anterior STG and the inferior frontal cortex, in addition to those described recently for auditory processing of vocalizations and speech (Ethofer et al., 2012; Glasser and Rilling, 2008;

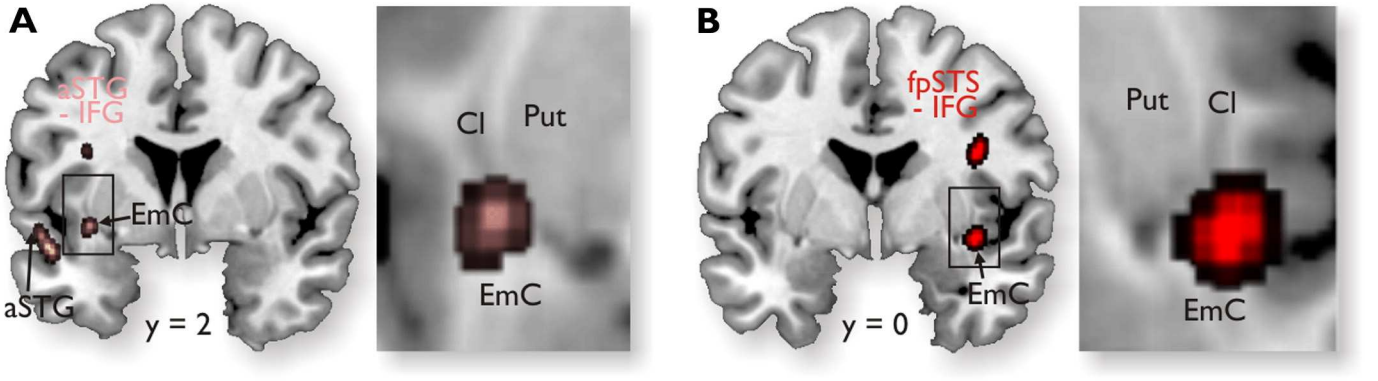

Fig. 5. Coronal view of the left and right ventral pathway. (A) The anterior part of the left ventral pathway for the connection between aSTG and IFG consisted primarily of fiber bundles of the left extreme capsule (EmC) lateral to the claustrum (Cl). The right panel shows an enlarged view of the EmC, Cl, and the putamen (Put) marked by the black box in the left panel. (B) The anterior part of the right ventral pathway connecting fpSTS and right IFG also consisted primarily of the EmC. The right panel shows an enlarged view of the area marked by the black box in the left panel.

Table 1
Microstructural properties of fiber tracks for the left and the right hemisphere. Fractional anisotropy (FA) is dimensionless, while mean diffusivity (MD) is given in the unit of 10^{-3} mm^2/s. Values in brackets indicate the standard error of the mean (SEM).

		FA		MD	
		fOP	IFG	fOP	IFG
Left	pSTG	0.364 (0.007)	0.370 (0.006)	0.774 (0.009)	0.764 (0.007)
	PPo	0.374 (0.008)	0.373 (0.006)	0.757 (0.009)	0.754 (0.007)
	aSTG	0.382 (0.006)	0.372 (0.007)	0.771 (0.009)	0.786 (0.008)
Right	fpSTS	0.372 (0.008)	0.380 (0.006)	0.762 (0.007)	0.767 (0.007)
	pSTG	0.370 (0.007)	0.372 (0.007)	0.754 (0.008)	0.769 (0.011)
	mSTG	0.365 (0.007)	0.365 (0.009)	0.761 (0.009)	0.796 (0.024)
	PPo	0.373 (0.006)	0.373 (0.008)	0.761 (0.010)	0.785 (0.021)

Rauschecker and Scott, 2009; Saur et al., 2008). The results are also indicative of dorsal and ventral temporo-frontal connections in the right hemisphere, especially of a previously not exhaustively described right ventral pathway (Ethofer et al., 2012). For the latter, we now provide quantitative description as well as evidence for the specific subregions in STC and IFC, which are structurally connected by the right ventral pathway. Second, we found an overall bilateral predominance of the dorsal pathway for processing affective prosody.

Concerning the left hemisphere, the ventral aSTG–IFG connection and the dorsal connection from the pSTG to the fOP resemble common connections for processing speech (Saur et al., 2008) probably because of the speech-likeness of the stimuli. These ventral and dorsal pathways specifically might decode the emotional meaning and the temporal prosody contour, respectively, in accordance with the more general view that the ventral pathway connects regions involved in processing sound meaning, and that the dorsal pathway connects regions involved in processing of temporal sound patterns (Rauschecker and Scott, 2009). However, the remaining left dorsal connection that especially targeted the IFG has not yet been described within the speech processing network, because these speech pathways are assumed to terminate in posterior frontal cortex (Friederici, 2011; Saur et al., 2008). Therefore, the dorsal connections to the anterior frontal cortex might be rather used for processing prosody superimposed on speech than speech itself, which is also corroborated by a functional connection between these areas (Fruhholz and Grandjean, 2012).

Thus, fiber connections from the STG via the dorsal pathway can terminate both in the posterior fOP as shown by speech processing studies (Saur et al., 2008), but also in the anterior IFG around BA 45 as shown here (see also Petrides et al., 2012; Rilling et al., 2008). Accordingly, we found connections both to fOP and IFG. Both regions have a strong sensitivity to affective prosody (Fruhholz and Grandjean, 2013b), and this sensitivity seems largely independent of acoustic features, and appear during both attention conditions (Fig. 1), indicating a general sensitivity to affective prosody, but with possible differences in their functional roles. The IFG is thought to evaluate (Schirmer and Kotz, 2006) and the fOP to categorize emotional cues related to prosody features (Romo et al., 2004).

The results in the right hemisphere provide interesting findings especially for the most posterior temporal regions in the posterior STS and STG (i.e. the fpSTS and the pSTG). Recent studies suggested that the right pSTG might be connected to the ipsilateral IFC via connections along the dorsal pathway (Ethofer et al., 2012; Glasser and Rilling, 2008). Here we provide the additional finding that the pSTG is dorsally connected specifically to the right fOP. This dorsal connection was not restricted to the pSTG since all STG seed regions showed a connection to the fOP. Interestingly, the left mSTG showed the least probable connection to the right fOP. In general, we found that the right IFG is strongly sensitive to prosody during implicit attention, while the mSTG is mainly active during explicit attention. This differential sensitivity to prosody might be explained by this relatively smaller connection probability between the mSTG and the fOP. Unlike the mSTG, all other temporal seed regions were active during implicit attention, similar to the left fOP, and accordingly show a strong connection probability to the fOP. The strong anatomical connectivity might explain their similar sensitivity to affective prosody.

Beside the right pSTG, the temporal region in the posterior fundus of the right STS (fpSTS) showed the strongest connection strength to frontal target regions, both along the right dorsal and ventral pathway. The fpSTS was the only region to target the right IFG, taking the right ventral pathway, which has been not well described in humans yet, but seems to have precursors in nonhuman primates (Ghazanfar, 2008; Rilling et al., 2008). Previously, we found that the fpSTS is active independent of the attentional focus, but exhibiting sensitivity to the features of acoustic features of affective prosody, such as pitch and intensity variations. Thus, the connection between the fpSTS and the IFG could support an evaluation of affective prosody on the basis of acoustic features decoded by the fpSTS and fed forward to the IFG, particularly during implicit attention, for which a functional connection was reported recently (Fruhholz and Grandjean, 2012). Unlike the right IFG, the right fOP was exclusively targeted by temporal seed region via the dorsal pathway. The fOP might be more responsible for the cognitive categorization and evaluation of affective prosody in support of response preparations (Romo et al., 2004) on the basis of higher-level prosody representations in the mSTG, which shows less acoustic sensitivity to pitch and intensity variations, but more sensitivity especially during explicit attention.

The right fOP was exclusively targeted by temporal seed region via the dorsal pathway, and we generally found a predominance of these dorsal pathways across both hemispheres. This predominance of the dorsal pathway is probably indicative of the processing of the temporal dynamics (Rauschecker and Scott, 2009) as an important cue for the decoding of affective prosody (Banse and Scherer, 1996; Belin and Zatorre, 2000b; Fruhholz et al., 2012). However, the dorsal pathway revealed some hemispheric differences in terms of termination on frontal target regions, particularly for those temporal seed regions that were common to both hemispheres (i.e. PPo, pSTG). While for these common left and right temporal seed regions the dorsal pathway exclusively targeted the fOP on the right hemisphere, they targeted both the fOP and the IFG in the left hemisphere. This probably points to a differential role of the left and right dorsal pathway in processing segmental and suprasegmental affective prosody, respectively (Fruhholz and Grandjean, 2013b), such that the dorsal pathway connection for segmental prosody additionally might target more anterior frontal regions in the left hemisphere.

In our study we have tested the probabilistic fiber pathway connectivity between the affective prosody responsive regions as obtained by fMRI, but it is possible that the described temporo-frontal fiber pathways do not display exclusivity for affective prosody processing only. Here, we have shown that these fiber pathways were the anatomical substrate of the distributed neural network for the decoding of affective prosody (Fruhholz and Grandjean, 2012, 2013b). However, since we have not directly compared this anatomical prosody network with other specific networks, especially the semantic language processing network, we cannot rule out the possibility that some of the connections also underlie other speech-related, or even general auditory functions. For example, some aspects of speech processing also involve the right hemisphere (Cogan et al., 2014; Hickok and Poeppel, 2007). Further studies are thus needed to determine if the anatomical connections described here are specific for affective prosody processing only, or if they are shared for the processing of other auditory stimuli. Taken together, our data show that both the left and the right hemisphere use the dorsal and the ventral pathway to process affective prosody, which imply three important findings. First, the dorsal and ventral connections might partly be used for different functions according to the feature-based decoding of affective prosody and according to the attention condition. Left IFG subregions responded both during the explicit and implicit attention condition, but left aSTG was more responsive during explicit attention and left PPo and pSTG more during implicit attention.

Thus, different left hemispheric STG to IFG connections might have stronger weight during each attention condition. Right STG to IFG connections might have a strong weight especially during the implicit attention condition due to the strong response of the right IFG during the implicit condition. Second, the temporal seed regions seem to largely originate in the temporal cortex with unique local white fiber bundles, which however unite at the level of the AF to form a single dorsal pathway together with the SLF. The ventral pathway in its major part consisted of the ILF, the IFOF and the EmC. These results are in accordance with recent general descriptions of both pathways (Friederici, 2011; Ghazanfar, 2008; Saur et al., 2008). We provide further a more detailed description especially of a right ventral pathway, which has been described only marginally for auditory processing in general (Gharabaghi et al., 2009; Makris and Pandya, 2009) and not exhaustively for affective prosody processing in specific (Ethofer et al., 2012; Glasser and Rilling, 2008). For the latter, especially an exact definition of the IFC subregions as one end of the ventral pathway was missing that could be only provided by bidirectional STC–IFC fiber tracking. Third and finally, we found an overall bilateral predominance of the dorsal pathway, which might support the strong processing of temporal pitch and intensity dynamics in regions connected by this pathway, these acoustic cues are important for the decoding of affective prosody (Banse and Scherer, 1996; Belin and Zatorre, 2000b; Patel et al., 2011). The latter might extend recent dual-stream models assuming a leftward dominance of the dorsal pathways (Hickok and Poeppel, 2007) by pointing to an important role of bilateral and especially of the *right* dorsal pathway for affective prosody processing.

We have to include a final note of caution concerning the unbalanced ratio of male and female participants in the final sample of participants. The results thus might be more valid for female than for male participants. Some studies have reported gender differences in terms of functional activations in response to affective prosody (e.g. Schirmer et al., 2004), but no evidence was reported so far for structural differences between male and female participants in neural language and para language network (e.g. Ethofer et al., 2012; Saur et al., 2008). However, for almost all of our resulting STC–IFC fiber connections, which were thresholded to be present in at least eight out of the 15 participants, all three male contributed to the fiber pathways. For two fiber connections (left PPo–IFG, right mSTG–fOP), only two of the three male participants contributed to the pathway. Thus, the STC–IFC structural network reported in the present study is likely to be valid both for female and male participants.

Acknowledgments

Grant funding was provided by the Swiss National Science Foundation (SNSF 105314_124572/1—DG) and by the NCCR in Affective Sciences at the University of Geneva (51NF40-104897—DG). All authors declare to have no conflict of interests.

References

Alba-Ferrara, L., Hausmann, M., Mitchell, R.L., Weis, S., 2011. The neural correlates of emotional prosody comprehension: disentangling simple from complex emotion. PLoS ONE 6, e28701.
Banse, R., Scherer, K.R., 1996. Acoustic profiles in vocal emotion expression. J. Pers. Soc. Psychol. 70, 614–636.
Beaucousin, V., Lacheret, A., Turbelin, M.R., Morel, M., Mazoyer, B., Tzourio-Mazoyer, N., 2007. FMRI study of emotional speech comprehension. Cereb. Cortex 17, 339–352.
Behrens, T.E., Berg, H.J., Jbabdi, S., Rushworth, M.F., Woolrich, M.W., 2007. Probabilistic diffusion tractography with multiple fibre orientations: what can we gain? Neuroimage 34, 144–155.
Belin, P., Zatorre, R.J., 2000a. Voice-selective areas in human auditory cortex. Nature 403, 309.
Belin, P., Zatorre, R.J., 2000b. 'What', 'where' and 'how' in auditory cortex. Nat. Neurosci. 3, 965–966.
Catani, M., Thiebaut de Schotten, M., 2008. A diffusion tensor imaging tractography atlas for virtual in vivo dissections. Cortex 44, 1105–1132.
Cogan, G.B., Thesen, T., Carlson, C., Doyle, W., Devinsky, O., Pesaran, B., 2014. Sensory-motor transformations for speech occur bilaterally. Nature 507, 94–98.
Croxson, P.L., Johansen-Berg, H., Behrens, T.E., Robson, M.D., Pinsk, M.A., Gross, C.G., Richter, W., Richter, M.C., Kastner, S., Rushworth, M.F., 2005. Quantitative investigation of connections of the prefrontal cortex in the human and macaque using probabilistic diffusion tractography. J. Neurosci. 25, 8854–8866.
de Wit, S., Watson, P., Harsay, H.A., Cohen, M.X., van de Vijver, I., Ridderinkhof, K.R., 2012. Corticostriatal connectivity underlies individual differences in the balance between habitual and goal-directed action control. J. Neurosci. 32, 12066–12075.
Ethofer, T., Anders, S., Erb, M., Herbert, C., Wiethoff, S., Kissler, J., Grodd, W., Wildgruber, D., 2006. Cerebral pathways in processing of affective prosody: a dynamic causal modeling study. Neuroimage 30, 580–587.
Ethofer, T., Bretscher, J., Gschwind, M., Kreifelts, B., Wildgruber, D., Vuilleumier, P., 2012. Emotional voice areas: anatomic location, functional properties, and structural connections revealed by combined fMRI/DTI. Cereb. Cortex 22, 191–200.
Friederici, A.D., 2011. The brain basis of language processing: from structure to function. Physiol. Rev. 91, 1357–1392.
Friederici, A.D., Bahlmann, J., Heim, S., Schubotz, R.I., Anwander, A., 2006. The brain differentiates human and non-human grammars: functional localization and structural connectivity. Proc. Natl. Acad. Sci. U. S. A. 103, 2458–2463.
Fruhholz, S., Grandjean, D., 2012. Towards a fronto-temporal neural network for the decoding of angry vocal expressions. Neuroimage 62, 1658–1666.
Fruhholz, S., Grandjean, D., 2013a. Multiple subregions in superior temporal cortex are differentially sensitive to vocal expressions: a quantitative meta-analysis. Neurosci. Biobehav. Rev. 37, 24–35.
Fruhholz, S., Grandjean, D., 2013b. Processing of emotional vocalizations in bilateral inferior frontal cortex. Neurosci. Biobehav. Rev. 37, 2847–2855.
Fruhholz, S., Ceravolo, L., Grandjean, D., 2012. Specific brain networks during explicit and implicit decoding of emotional prosody. Cereb. Cortex 22, 1107–1117.
Gharabaghi, A., Kunath, F., Erb, M., Saur, R., Heckl, S., Tatagiba, M., Grodd, W., Karnath, H.O., 2009. Perisylvian white matter connectivity in the human right hemisphere. BMC Neurosci. 10, 15.
Ghazanfar, A.A., 2008. Language evolution: neural differences that make a difference. Nat. Neurosci. 11, 382–384.
Glasser, M.F., Rilling, J.K., 2008. DTI tractography of the human brain's language pathways. Cereb. Cortex 18, 2471–2482.
Gschwind, M., Pourtois, G., Schwartz, S., Van De Ville, D., Vuilleumier, P., 2012. White-matter connectivity between face-responsive regions in the human brain. Cereb. Cortex 22, 1564–1576.
Hagoort, P., 2005. On Broca, brain, and binding: a new framework. Trends Cogn. Sci. 9, 416–423.
Hickok, G., Poeppel, D., 2007. The cortical organization of speech processing. Nat. Rev. Neurosci. 8, 393–402.
Hua, K., Zhang, J., Wakana, S., Jiang, H., Li, X., Reich, D.S., Calabresi, P.A., Pekar, J.J., van Zijl, P.C., Mori, S., 2008. Tract probability maps in stereotaxic spaces: analyses of white matter anatomy and tract-specific quantification. Neuroimage 39, 336–347.
Makris, N., Pandya, D.N., 2009. The extreme capsule in humans and rethinking of the language circuitry. Brain Struct. Funct. 213, 343–358.
Patel, S., Scherer, K.R., Bjorkner, E., Sundberg, J., 2011. Mapping emotions into acoustic space: the role of voice production. Biol. Psychol. 87, 93–98.
Petrides, M., Tomaiuolo, F., Yeterian, E.H., Pandya, D.N., 2012. The prefrontal cortex: comparative architectonic organization in the human and the macaque monkey brains. Cortex 48, 46–57.
Pierpaoli, C., Jezzard, P., Basser, P.J., Barnett, A., Di Chiro, G., 1996. Diffusion tensor MR imaging of the human brain. Radiology 201 (3), 637–648.
Rauschecker, J.P., Scott, S.K., 2009. Maps and streams in the auditory cortex: nonhuman primates illuminate human speech processing. Nat. Neurosci. 12, 718–724.
Rilling, J.K., Glasser, M.F., Preuss, T.M., Ma, X., Zhao, T., Hu, X., Behrens, T.E., 2008. The evolution of the arcuate fasciculus revealed with comparative DTI. Nat. Neurosci. 11, 426–428.
Romo, R., Hernandez, A., Zainos, A., 2004. Neuronal correlates of a perceptual decision in ventral premotor cortex. Neuron 41, 165–173.
Saur, D., Kreher, B.W., Schnell, S., Kummerer, D., Kellmeyer, P., Vry, M.S., Umarova, R., Musso, M., Glauche, V., Abel, S., Huber, W., Rijntjes, M., Hennig, J., Weiller, C., 2008. Ventral and dorsal pathways for language. Proc. Natl. Acad. Sci. U. S. A. 105, 18035–18040.
Schirmer, A., Kotz, S.A., 2006. Beyond the right hemisphere: brain mechanisms mediating vocal emotional processing. Trends Cogn. Sci. 10, 24–30.
Schirmer, A., Zysset, S., Kotz, S.A., Yves von Cramon, D., 2004. Gender differences in the activation of inferior frontal cortex during emotional speech perception. Neuroimage 21, 1114–1123.
Smith, S.M., Jenkinson, M., Johansen-Berg, H., Rueckert, D., Nichols, T.E., Mackay, C.E., Watkins, K.E., Ciccarelli, O., Cader, M.Z., Matthews, P.M., Behrens, T.E., 2006. Tract-based spatial statistics: voxelwise analysis of multi-subject diffusion data. Neuroimage 31, 1487–1505.
Specht, K., 2014. Neuronal basis of speech comprehension. Hear. Res. 307, 121–135.
Wahl, M., Li, Y.O., Ng, J., Lahue, S.C., Cooper, S.R., Sherr, E.H., Mukherjee, P., 2010. Microstructural correlations of white matter tracts in the human brain. Neuroimage. 51, 531–541.